Journal of Innovation and Development
ISSN: 2958-4752 | Vol. 10, No. 2, 2025

Analysis of Welding Simulation Methods for Large Weldments

Sheng Wu[1, 2, a], Xing Liu[1, 2], Youli Yao[1], Jing Mei[1, 2], Xianyong Zeng[1, 2]

[1]School of Mechanical Engineering, Sichuan Vocational College of Chemical Technology, Luzhou, 646300, China
[2]The Key Laboratory of Mechanical Structure Optimization &Material Application Technology of Luzhou, Luzhou, 646300, China
[a]1077466992@qq.com

Abstract: In response to the problems of long simulation time and low efficiency in the optimization process of welding process parameters for large welded parts, this paper analyzes the application of the birth and death element method and the non birth and death element method in the circumferential weld of ball valves using fully welded ball valves as carriers. The difference between the two methods in the key indicators of residual stress and deformation after welding is 17.8% and 6%, respectively, and the distribution pattern is consistent. Moreover, the birth and death element method is more in line with the actual process. Based on the analysis results, the large birth and death element method was proposed to simulate the welding process. The simulation results showed that using the large birth and death element method can improve the simulation efficiency by 28% and 12.5% respectively compared to the birth and death element method and non birth and death element method, while ensuring the accuracy of the welding simulation results.

Keywords: Welding method, birth death element method, residual stress, efficiency.

1. Introduction

The optimization of welding process parameters for welded parts has always been a hot topic of research, generally through experimental and simulation methods. However, for large welded parts, the cost of using experimental methods is too high, and enterprises find it difficult to afford in the actual production process. Therefore, for the optimization of process parameters for large welded parts, simulation is generally used first to optimize the process parameters, and then the process parameters are verified.

Lin Haitao et al. established a numerical model for the relationship between welding current, angle, speed, and weld morphology of large valves by studying the influence of welding parameters and single welds. They then used genetic algorithm to optimize the model and finally obtained the optimal welding process parameters, which showed high accuracy in experiments. Wang Tianqi used genetic algorithm combined with neural network to establish a process prediction method and optimization measures for multi-layer and multi pass welding. Through this method, real-time prediction of welding process parameters and weld morphology can be made to make timely improvement measures. Finally, the feasibility of the method was verified through experiments. Regarding the optimization of process parameters for double wire three arc welding, Ma Zhen et al. used response surface methodology to establish the relationship between wire current, arc voltage, welding dilution rate, and welding current, and completed the optimization design. Chen Wenjie et al. aimed to address the issue of high welding stress in large connecting pipes of reactor pressure vessels. They established a finite element numerical model and used orthogonal experimental method to analyze the relationship between welding parameters and residual stresses after welding. They determined sensitive parameters and then combined genetic algorithm for parameter optimization.

It is not difficult to find from the analysis of current research that most of the methods used are to first establish the relationship between welding process parameters and post weld stress, deformation, etc., train a surrogate model using a large number of finite element calculation results, and then optimize the parameters through genetic algorithms or experimental methods, ultimately obtaining optimized parameters. However, in the current process of training models, a large amount of finite element analysis data is required, which requires a significant amount of time. In the welding simulation process, there are two main methods used: the birth and death element method and the non birth and death element method. The birth and death element method considers the influence of elements on the entire welding process. Firstly, the weld element is invalidated as a whole, that is, the element is killed. Then, as the welding process progresses, the element is gradually activated, that is, the element is regenerated, to accurately simulate the welding behavior; The non birth and death element method does not consider the influence of elements, but only considers the influence of the heat source on the entire welding process to shorten the calculation time. This article will use a large fully welded forged steel ball valve as a carrier to explore the effects of two welding methods on the welding of large deep narrow ring welds.

2. Analysis and Calculation Theory

2.1. Differential equation of heat conduction and steady-state heat transfer process

The welding process is a dynamic thermal conduction process of an object, and the entire process of heat conduction until the heat reaches a thermal equilibrium state satisfies the principle of energy conservation. Assuming there is an isotropic and uniform material with a unit volume heat source of Qv, the differential equation for heat conduction is as follows:

$$\frac{\partial T}{\partial t}=\frac{\lambda}{cp}\left(\frac{\partial^2 T}{\partial x^2}+\frac{\partial^2 T}{\partial y^2}+\frac{\partial^2 T}{\partial z^2}\right)+\frac{1}{c\rho}\frac{\partial Q_v}{\partial t} \quad (1)$$

Among them, c, ρ, and λ are the specific heat capacity, density, and thermal conductivity of the material, respectively, and T is the temperature of the object. If a=λ/cp, then a is called the thermal diffusion coefficient. After the thermal conduction process is completed and gradually stabilizes, T=0, The above equation can be simplified as:

$$\lambda\left(\frac{\partial^2 T}{\partial x^2}+\frac{\partial^2 T}{\partial y^2}+\frac{\partial^2 T}{\partial z^2}\right)+\frac{\partial^2 Q_v}{\partial z}=0 \quad (2)$$

From the above equation, it can be seen that when the heat transfer system reaches the equilibrium heat conduction state, the thermal diffusion coefficient has no effect on the heat transfer system, but the thermal conductivity coefficient λ of the object has an impact on the heat transfer system. Further analysis shows that if there is no heat source inside the heat transfer system at this time, equation (1) can be further simplified as:

$$\frac{\partial^2 T}{\partial x^2}+\frac{\partial^2 T}{\partial y^2}+\frac{\partial^2 T}{\partial z^2}=\nabla^2 T=0 \quad (3)$$

When the system is in a thermally stable equilibrium state, its net heat flow rate is zero. At this point, the equilibrium equation for thermal steady state is as follows:

$$[K]\bullet\{T\}=\{Q\} \quad (4)$$

In the above equation, [K] represents the thermal conductivity matrix of the entire thermal conductive object, {T} represents the temperature vector of each unit node, and {Q} represents the thermal vector of each unit node.

2.2. Nonlinear transient heat conduction analysis theory

The heat conduction of welding is a transient and highly nonlinear process, and with the local variation of the heat source, uneven temperature gradients will appear in the local area of the welding material, and phase transitions will also occur with the melting process of the material. Therefore, as the welding process changes, there is a high degree of inconsistency in the heating, phase transformation, and cooling processes, and the heat conduction control equation for this process is shown in Equation 1.

$$\rho c\frac{\partial T}{\partial t}=\frac{\partial}{\partial x}\left(\lambda\frac{\partial T}{\partial x}\right)+\frac{\partial}{\partial y}\left(\lambda\frac{\partial T}{\partial y}\right)+\frac{\partial}{\partial z}\left(\lambda\frac{\partial T}{\partial z}\right)+\overline{Q} \quad (5)$$

In the formula, ρ represents the material density, c is the specific heat capacity of the material, λ is the thermal conductivity of the material, T represents the distribution function of a specific temperature field, $\bar{Q}$ is the strength of the internal heat source during welding, and t is the welding heat transfer time.

It is generally solved using heat flux density boundary conditions and convective heat transfer boundary conditions, as shown in equations 2 and 3, respectively.

$$-\lambda\left(\frac{\partial t}{\partial n}\right)_w=f_2(\tau),\quad \tau>0 \quad (6)$$

$$-\lambda\left(\frac{\partial t}{\partial n}\right)_n=h(t_w-t_f) \quad (7)$$

In the formula, n represents the normal direction of the contact surface with the heat source, h represents the surface heat transfer coefficient between the thermal boundary and the surrounding heat-conducting objects, and tf is the temperature of the fluid medium.

3. Analyze and Calculate the Model

Large fully welded forged steel ball valves are mainly used on long-distance oil and gas pipelines for fluid control in valve stations. Their structure is shown in Figure 1. After the internal parts are installed, they are welded from three parts: the left body, right body, and middle body. No heat treatment measures are taken after welding, so they have high requirements for welding process parameters. The DN40 "FW-WE-600LB large-diameter fully welded forged steel ball valve studied in this article is independently developed by China. Its weld size is shown in Figure 2, with a weld depth of 71.5mm, width of 16mm, and taper of 2 °. It is a typical large deep narrow annular weld. Due to the inability to heat treat after welding, the deformation of the left and right bodies caused by welding should not be too large, otherwise it will cause ball rotation failure. Additionally, the temperature transmitted to the valve seat due to welding should not be too high, otherwise it will damage the lubricating medium and non-metallic seals in the contact area between the valve seat and the ball. The material used for the left and right bodies as well as the middle body of the ball valve is A350-LF2, and the physical properties of the material are shown in Table 1.

The fully welded forged steel pipeline ball valve is composed of three parts: the left body, the right body, and the middle body. The welds between each part are welded using narrow gap submerged arc automatic welding. The interior of the ball valve must withstand high pressure, and the weld depth is 71.5 mm. Multi layer periodic welding technology is used, and the initial welding process parameters are as follows: welding current is 380 A, welding voltage is 32 V, welding cycle is 960 s, single-layer weld thickness is 5 mm, a total of 14 layers of welds.

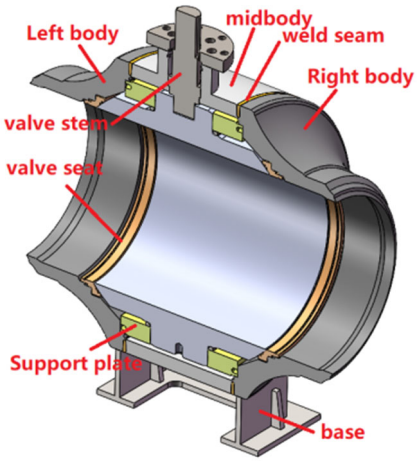

Figure 1. Structure of fully welded ball valve

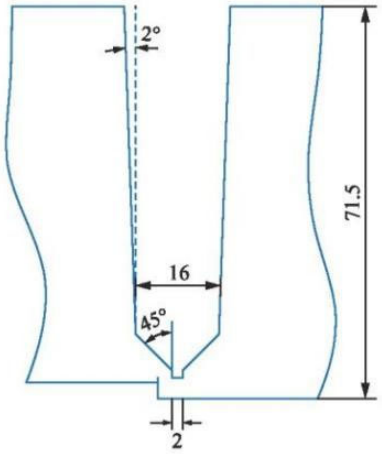

Figure 2. Weld seam size

Table 1. Thermophysical Properties Parameters of A350-LF2 Steel

Temperature °C	Thermal conductivity/ $W \cdot m^{-1} \cdot K^{-1}$	Density/ $kg \cdot m^{-3}$	Young's modulus MPa	Poisson's ratio	coefficient of expansion/°C	yield stress/ MPa	specific heat capacity/ $J \cdot g^{-1} \cdot K^{-1}$
20	45	7800	205	0.28	1.32e-5	390	450
200	40	7700	195	0.29	1.35e-5	355	500
400	38	7600	180	0.30	1.45e-5	300	580
600	30	7550	155	0.31	1.60e-5	140	625
800	34	7500	105	0.31	1.40e-5	50	630
1000	37	7400	85	0.33	1.38e-5	20	625
1300	42	7300	30	0.36	1.42e-5	20	630
1500	55	7250	80	0.35	1.4e-5	20	640

4. Comparison of Analysis and Calculation Methods

In the welding process, the parameters that people are mainly concerned about include welding stress distribution, residual stress after welding, and deformation after welding. This article will compare the differences in the above parameters between the birth and death element method and the non birth and death element method to comprehensively evaluate the advantages and disadvantages of the two methods. Using ABAQUS software combined with Python for secondary development, welding simulations were conducted separately. The welding process was loaded with a double ellipsoid heat source model, and the simulation process is shown in Figure 3. The calculation model is shown in Figure 4.

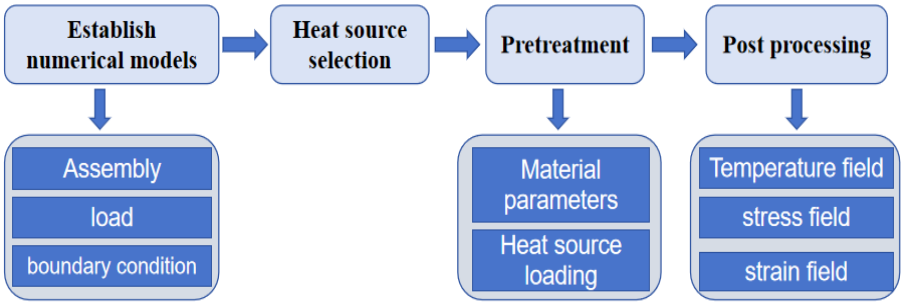

Figure 3. Simulation Process

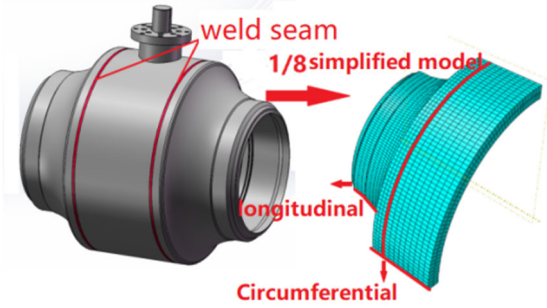

Figure 4. Analysis and Calculation Model

4.1. Welding stress distribution

The simulation of ball valve welding was carried out using the birth and death element method and non birth and death element method. The stress distribution after welding is shown in Figure 5. To visually analyze the stress distribution of the ball valve, the stress cloud map displays the 1/2 model symmetrically.

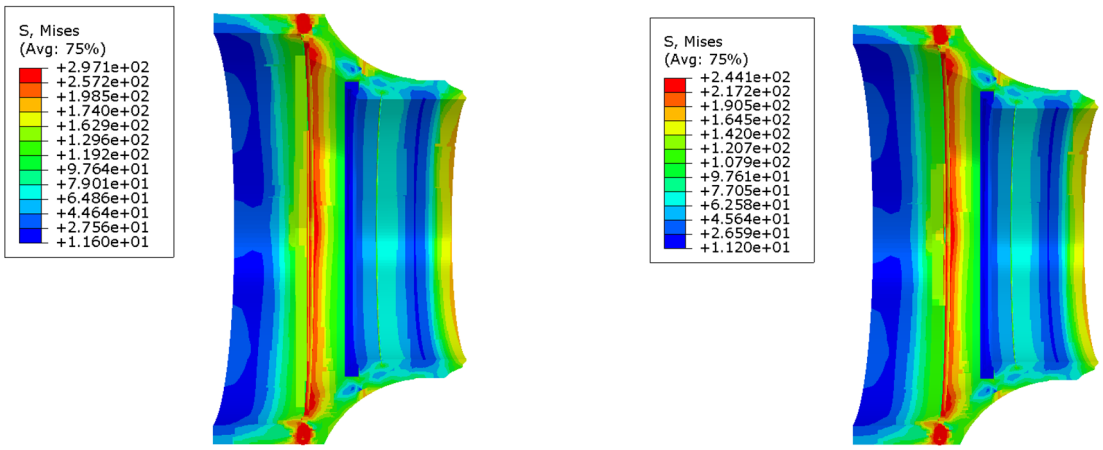

(a) Life and Death Unit Method (b) Non Life and Death Unit Method

Figure 5. Stress simulation results

From the perspective of overall stress distribution, the stress distribution pattern is similar. In terms of circumferential stress, the middle of the ball valve is subjected to tensile stress. As it approaches the weld area, the tensile stress gradually decreases and fluctuates in the weld area. The right side of the ball valve near the weld is subjected to compressive stress, which gradually decreases and transforms into tensile stress as the distance from the weld area increases. As for axial stress, the middle part of the ball valve also experiences tensile stress, but its variation trend is opposite to circumferential stress, that is, as it approaches the weld area, the tensile stress gradually increases. After entering the affected area of the weld, the tensile stress rapidly decreases and there is a fluctuation in compressive stress. The axial stress variation trend on the right side of the ball valve is consistent with the circumferential stress. Numerically speaking, the use of the birth death element method results in a larger residual stress difference of 53 Mpa compared to the non birth death element method, with a difference of approximately 17.8%. This is because the birth death element method gradually activates the elements as the weld seam is formed, causing discontinuities in material distribution, heat conduction, and other aspects, resulting in more pronounced stress changes that are more in line with actual production.

4.2. Distribution of Welding Deformation

By analyzing the deformation of the ball valve, we found that due to uneven distribution of internal stress, plastic deformation occurred in the weld area. The deformation vector diagram of the ball valve is shown in Figure 6, where the direction of the arrow represents the direction of deformation contraction, and the length and color of the arrow represent the magnitude of displacement. The longer the arrow and the darker the color, the greater the deformation. From the figure, it can be observed that under the combined action of circumferential stress and axial stress, the right and middle bodies of the ball valve shrink and deform towards the weld area. Based on the analysis of residual stress, we found that the shrinkage deformation of the right body of the ball valve is greater than that of the middle body, which is the main reason for the occurrence of shear stress at the weld position. The maximum deformation calculated using the birth and death element method is about 2.46 mm, while the maximum deformation obtained using the non birth and death element method is 2.31 mm, with a difference of about 6%.

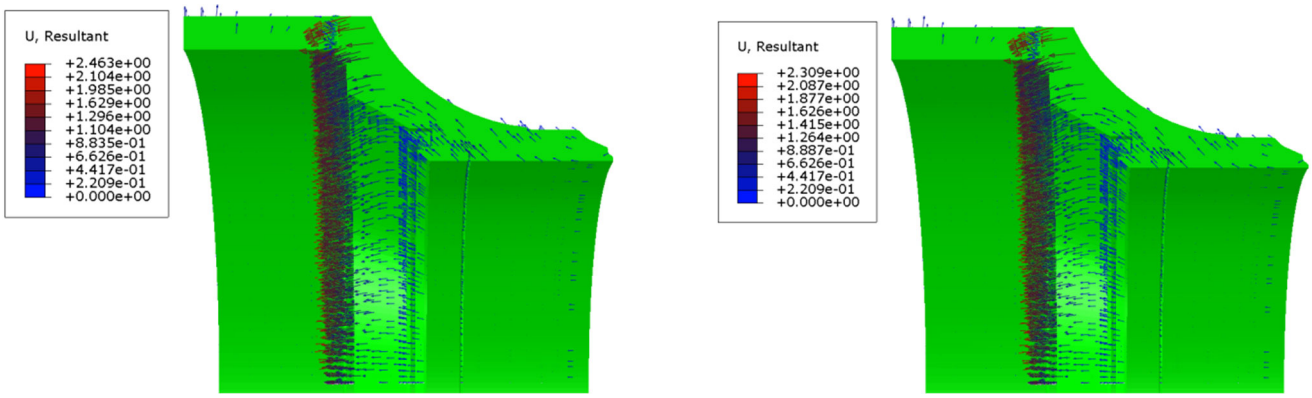

(a) Life and Death Unit Method (b) Non Life and Death Unit Method

Figure 6. Deformation simulation results

5. Optimization of Welding Process

Analyzing the key result parameters of the welding process mentioned above, it is not difficult to find that using the birth and death element method is cumbersome and complex, while using the non birth and death element method is simple and convenient. However, the birth and death element method is more in line with the actual welding process. Due to the existence of structural and material discontinuities, the stress and deformation after welding are greater than those of non birth and death elements. Therefore, based on the advantages and disadvantages of the two methods, a large birth and death element method is proposed, which treats one or more layers of welds as a large element and activates them sequentially during the welding process, considering both operational convenience and practical processing. Using the above method, in the welding process of the fully welded ball valve, taking layer 1 as a large unit, the distribution of post weld stress and deformation is shown in Figure 7.

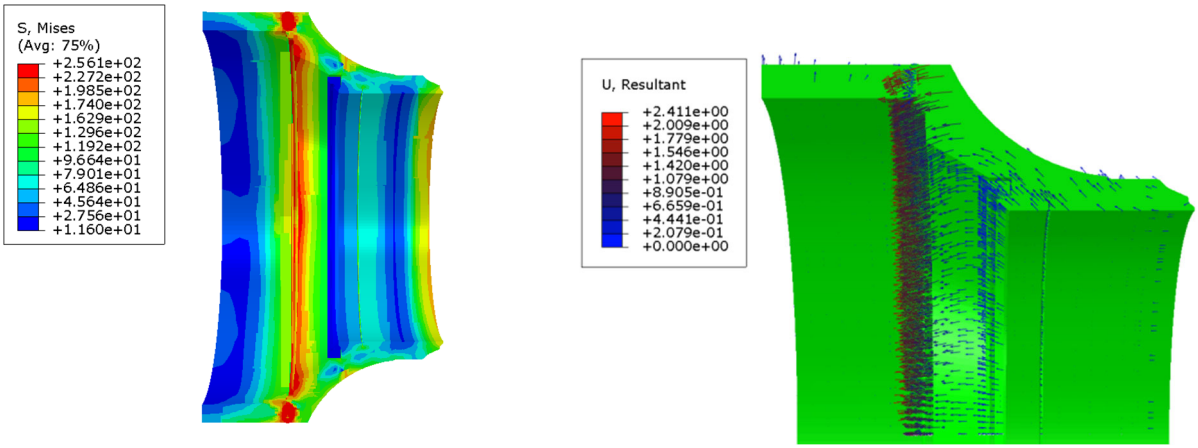

(a) Post weld residual stress (b) post weld deformation

Figure 7. The method of major life and death units

According to Figure 7, it can be seen that using the large birth and death element method for welding simulation results in the same residual stress distribution and deformation distribution after welding as the birth and death element method and the non birth and death element method, but there is a certain difference in numerical values, which is consistent with the above reasons. Compared with the same birth and death element method, the large birth and death element method has a residual stress and deformation change rate of -14.8% and -2% after welding, respectively; Compared with the non birth and death element method, the large birth and death element method has a residual stress and deformation change rate of 5% and 5% after welding, respectively.

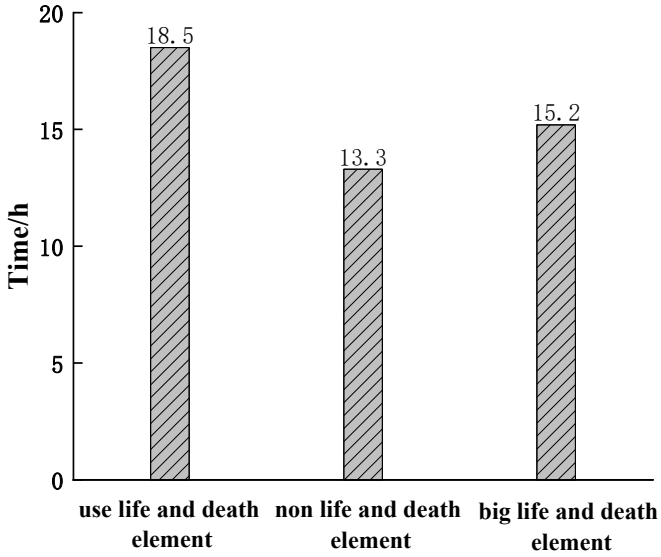

Figure 8. Comparison of Welding Efficiency

In practical applications, especially when calculating large and complex components, in addition to ensuring calculation accuracy, calculation efficiency is also an important evaluation indicator. The comparison of welding time using three methods is shown in Figure 8. The non birth and death element method has simpler pre-processing settings and requires much less computation time than the birth and death element method. Moreover, the larger the calculation component size and the more complex the structure, the more obvious the computational efficiency advantage it exhibits. The proposed large birth and death element method can improve computational efficiency and shorten computation

time while considering accuracy.

6. Summary

(1) The use of the birth and death element method to simulate the welding process is more in line with actual welding processing. Due to the existence of structural and material discontinuities, the simulation results are higher than those of the non birth and death element method. The difference in residual stress and deformation in welding between the two methods is 17.8% and 6%, respectively.

(2) The distribution of welding residual stress is consistent with that of the birth and death element method and the non birth and death element method using the large birth and death element method. The welding residual stress and deformation are lower than those of the birth and death element method and higher than those of the non birth and death element method.

(3) The use of the large birth and death element method can effectively improve the efficiency of welding simulation while ensuring the accuracy of welding simulation results. Compared with the birth and death element method and the non birth and death element method, the efficiency is increased by 28% and 12.5% respectively.

7. Fund Project

Key R&D Project of Sichuan Provincial Department of Science and Technology (23ZDYF0492); Luzhou Science and Technology Bureau Science and Technology Innovation Seed Project (2023RCM188)

References

[1] Liu Xiaobao, Yan Qingxiu, Yao Tingqiang, et al. Optimization of process parameters based on ensemble learning and improved particle swarm optimization[J/OL] China Mechanical Engineering, 1-14 [2022-11-12].

[2] Yin Xiqin, Gao Zicheng, Li Lijun, etc Spindle Multi-objective Optimization Design Based on Response Surface and MOGA [J] Machine Tool & Hydraulics, 2024, 52 (12): 98-103+156.

[3] Wang Wang, Research on Optimization of Welding Process of Fully Welded Ball Valve Based on Thermal-mechanical Coupling Simulation and Physical Experiment [D] Sichuan University of Science & Engineering, 2021.

[4] Huang Bo, Wang Wang, Wang Jia, et al. Numerical simulation on welding residual stress and deformation of all-welded ball valves [J]Oil & Gas Storage and Transportation, 2021, 40 (08): 895-902.

[5] Lin Haitao, Yu Shengfu, Wang Hongyun, et al. Optimization of Process Parameters and Study on Mechanical Properties of Valve Ring Welding Based on Robot Welding [J/OL] Hot processing technology, 2025, (01): 33-38+44 [2024-11-12].

[6] Zhang Guizhi, Zhang Liping, and Zhan Xiaohong The influence of weld bead filling method on welding deformation and welding residual stress [J]. Welding Technology, 2017, 46 (10): 16-19. DOI: 0.13846/j.cnki.cn12-1070/tg.2017.10.004.

[7] Zhang Liang, Guo Yuli, Qi Lei The influence of weld bead filling method on numerical simulation of residual stress in X65 pipeline steel circumferential weld [J]. Welding Technology, 2020, 49 (06): 5-8. DOI: 10.13846/j.cnki. cn12-1070/tg.2020.06.002.

[8] Dai Hao, Han Haibo, Liu Xiangbo, etc Research on Finite Element Simulation and Process Optimization of Single Tube Exhaust Pipe Welding [J/OL]. Material Introduction, 1-7 [2022-12-18].

[9] Peng Fei, Wang Meng, Yang Xiuxiu, etc Finite element numerical simulation analysis and sequential optimization of welding of large vibrating screen beam [J]. Industrial Technology and Vocational Education, 2024, 22 (05): 9-13+43. DOI: 10.16825/j.cnki. cn13-1400/tb. 2024.05.021.

[10] Shen Wei, Guo Jiaxing, Yin Le Laser Welding Heat Source Simulation Optimization and Residual Stress Simulation Analysis [J/OL]. Journal of Jilin University (Engineering Edition), 1-9 [2024 -12-18]

[11] Chen Tianxi, Lu Lili, Lin Tengfei, etc Simulation of Welding Process of Titanium Alloy Tube Plate Based on ABAQUS [J]. Welding Machine, 2024, 54 (09): 96-104.

[12] Liu Congyue, Bu Mingzhe, Zhang Jie, etc Numerical simulation study on stress of pipeline welding joints in steep mountainous areas [J]. Welding Machine, 2024, 54 (08): 108-117.